

## Supporting Information

### **An Unprecedented Planar $\pi$ -conjugated [B<sub>2</sub>P<sub>5</sub>] Group with Ultra-large Birefringence and Nonlinearity: an *ab-initio* Study**

Pifu Gong,<sup>a</sup> Shengzi Zhang,<sup>a,c</sup> Gaomin Song,<sup>a,c</sup> Xiaomeng Liu,<sup>a,c</sup>  
Zheshuai Lin<sup>a,b,c\*</sup>

<sup>a</sup> *Technical Institute of Physics and Chemistry, Chinese Academy of Sciences, Beijing 100190 PR China*

<sup>b</sup> *Center of Materials Science and Optoelectronics Engineering, University of Chinese Academy of Sciences, Beijing 100049 PR China*

<sup>c</sup> *University of the Chinese Academy of Sciences, Beijing 100049 PR China*

## Contents

### 1. Computational methods

### 2. Experimental Procedures

3. **Table S1.** Comparison of the bandgaps and the largest SHG coefficients of the classic tetrahedra-base NLO sulfides and pnictides.

4. **Table S2.** Comparison of the bandgaps and the calculated SHG coefficients with and without structure optimization.

5. **Figure S1.** The calculated phonon spectrum for  $\text{Na}_2\text{BP}_2$ . The absence of imaginary frequency verifies the kinetic stability of the structure.

6. **Figure S2.** The calculated (a) IR, Raman spectrum and (b) the corresponding group vibrations for  $\text{Na}_2\text{BP}_2$ .

## Computational methods

The first-principles electronic structure calculations for Na<sub>2</sub>BP<sub>2</sub> are performed using the plane-wave pseudopotential method<sup>1</sup> implemented in CASTEP package<sup>2</sup> based on the density functional theory (DFT).<sup>3</sup> The optimized norm-conserving pseudopotentials<sup>4</sup> for all the elements are used, in which Na 2s<sup>2</sup>2p<sup>6</sup>3p<sup>1</sup>, B 2s<sup>2</sup>2p<sup>1</sup>, and P 3p<sup>2</sup>3p<sup>3</sup> electrons are treated as the valence electrons, respectively. The Perdew, Burke and Ernzerhof (PBE) functionals<sup>5</sup> of generalized gradient approximation (GGA) are adopted to describe the exchange-correlation (XC) functionals. The kinetic energy cutoffs of 900 eV and Monkhorst-Pack *k*-point meshes<sup>6</sup> with a density of 4×4×2 points in the Brillouin zone are chosen. Our tests reveal that the above computational set ups are sufficiently accurate for present purposes.

Based on the electronic structures, the imaginary part of the dielectric function is calculated and the real part of the dielectric function is determined using the Kramers– Kronig transform,<sup>7</sup> and then the refractive indices *n* and the birefringence Δ*n* are obtained. Moreover, the SHG coefficients *d<sub>ij</sub>* are obtained by the formula developed by Lin et al:<sup>8</sup>

$$\chi^{\alpha\beta\gamma} = \chi^{\alpha\beta\gamma} (VE) + \chi^{\alpha\beta\gamma} (VH) + \chi^{\alpha\beta\gamma} (twobands)$$

where

$$\chi^{\alpha\beta\gamma} (VE) = \frac{e^3}{2h^2m^3} \times \sum_{vcc'} \int \frac{d^3k}{4\pi^3} P(\alpha\beta\gamma) \text{Im} [p_{vc}^\alpha p_{cc'}^\beta p_{c'v}^\gamma] \left( \frac{1}{\omega_{cv}^3 \omega_{vc'}^2} + \frac{2}{\omega_{vc}^4 \omega_{c'v}} \right)$$

$$\chi^{\alpha\beta\gamma} (VH) = \frac{e^3}{2h^2m^3} \times \sum_{vv'c} \int \frac{d^3k}{4\pi^3} P(\alpha\beta\gamma) \text{Im} [p_{vv'}^\alpha p_{v'c}^\beta p_{cv}^\gamma] \left( \frac{1}{\omega_{cv}^3 \omega_{v'c}^2} + \frac{2}{\omega_{vc}^4 \omega_{cv'}} \right)$$

and

$$\chi^{\alpha\beta\gamma} (twobands) = \frac{e^3}{h^2m^3} \times \sum_{vc} \int \frac{d^3k}{4\pi^3} P(\alpha\beta\gamma) \frac{\text{Im} [p_{vc}^\alpha p_{cv}^\beta (p_{vv}^\gamma - p_{cc}^\gamma)]}{\omega_{vc}^5}$$

Here,  $\alpha, \beta,$  and  $\gamma$  are Cartesian components, *v* and *v'* denote valence bands, and *c* and *c'* denote conduction bands. *P*( $\alpha\beta\gamma$ ) denotes full permutation and explicitly shows the Kleinman symmetry of the SHG coefficients. The band energy difference and

momentum matrix elements are denoted as  $\hbar\omega_{ij}$  and  $p_{ij}^\alpha$ , respectively, and they are all implicitly  $k$  dependent.

Moreover, in order to analyze the contribution of an ion (or ionic group) to the  $n$ th order susceptibility  $\chi^{(n)}$ , a real-space atom-cutting technique is adopted.<sup>8</sup> Within this method the contribution of ion  $A$  to the  $n$ th-order susceptibility (denoted as  $\chi^{(n)}(A)$ ) is obtained by cutting all ions except  $A$  from the original wave functions  $\chi^{(n)}(A) = \chi^{(n)}$  (all ions except  $A$  are cut).

SHG-weighted electron density analysis is performed to identify the orbitals contributing the SHG most in the compound. In this scheme, the considered SHG coefficient is “resolved” onto each orbital, and then the SHG-weighted bands are used to sum the probability densities of all occupied (valence) or unoccupied (conduction) states. This ensures that the quantum states irrelevant to SHG are not shown in the occupied or unoccupied “SHG-densities,” while the orbitals vital to SHG are intuitively highlighted in the real space.

## **Experimental Procedures**

According to Reference 9, a ratio of 1:1  $\text{Na}_3\text{BP}_2$ : $\text{CuCl}$  was loaded in a silica ampoule in solid state oxidative elimination reactions. Once loaded, the ampoule was evacuated and flame sealed, and then placed in a muffle furnace. The heating profile includes ramping 1 h to 773 K and then dwelling at that temperature for 1 h. The sample was opened and stored in an argon filled glovebox. To synthesize  $\text{Na}_2\text{BP}_2$ , the 1:1  $\text{Na}_3\text{BP}_2$ : $\text{CuI}$  mixture was added to a mass equivalent of eutectic salt flux composed of 1:0.94  $\text{CsI}$ : $\text{NaI}$ . The ramp time for the flux reaction was increased to 3 h and dwell time was increased to 24 h.

For the diffuse reflectance spectroscopy, powder sample containing  $\text{Na}_2\text{BP}_2$  was pressed inside an Ar-filled glovebox onto a glass slide wrapped with Teflon tape and white filter paper. The sample was further sealed in a polyethylene bag inside the glovebox using a heat sealer. A BLACK-Comet C-SR-100 spectrometer was used to obtain UV-Vis diffuse reflectance data in the 250-1100 nm range.

**Table S1.** Comparison of the bandgaps and the calculated SHG coefficients of the classic tetrahedra-base NLO sulfides and pnictides. The calculated SHG coefficients for AgGaS<sub>2</sub> and ZnGeP<sub>2</sub> agree well with the experimental values, indicating the accuracy of our calculated method. Clearly, the NLO pnictides exhibit smaller bandgaps but larger SHG coefficients when comparing with the NLO sulfides in the same space groups.

Space Groups	Compounds	E <sub>g</sub> (eV)	<i>d</i> <sub>ij</sub> (pm/V)
I-4 <sub>2</sub> d	AgGaS <sub>2</sub>	2.7	<i>d</i> <sub>36</sub> =14.00
	ZnGeP <sub>2</sub>	2.0	<i>d</i> <sub>36</sub> =68.55
F-4 <sub>3</sub> m	CdS	2.6	<i>d</i> <sub>14</sub> =9.52
	GaP	2.2	<i>d</i> <sub>14</sub> =28.57
P6 <sub>3</sub> mc	Na <sub>6</sub> ZnS <sub>4</sub>	2.4	<i>d</i> <sub>33</sub> =3.86
	Na <sub>3</sub> Sr <sub>3</sub> GaP <sub>4</sub>	1.4	<i>d</i> <sub>33</sub> =19.35

**Table S2.** Comparison of the bandgaps and the calculated SHG coefficients with and without structure optimization. Clearly, the calculated bandgap without structure optimization exhibits better agreement with the experimental result, indicating the accuracy of the chosen parameters for the optical calculations.

	$E_g$ (eV)	$d_{ij}$ (pm/V)	$\Delta n$
Without structure optimization	1.37	$d_{12}=57.14$	0.68
Performed structure optimization	1.40	$d_{12}=55.66$	0.66

**Figure S1.** The calculated phonon spectrum for  $\text{Na}_2\text{BP}_2$ . The absence of imaginary frequency verifies the kinetic stability of the structure.

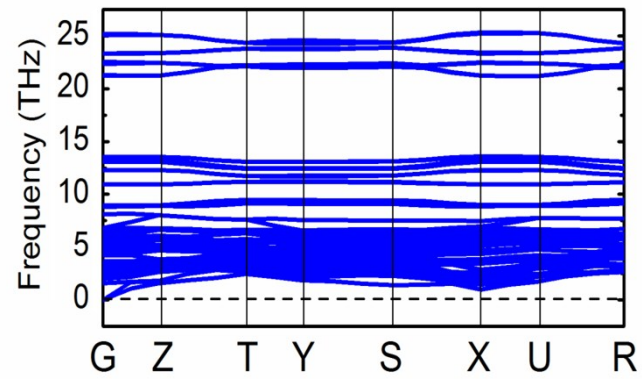
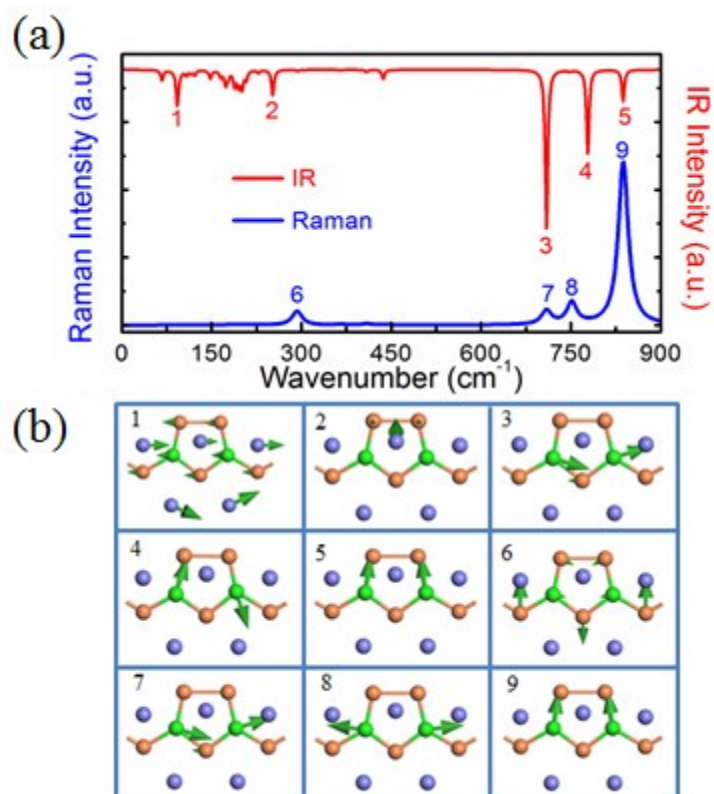




**Figure S2.** The calculated (a) IR, Raman spectrum and (b) the corresponding group vibrations for  $\text{Na}_2\text{BP}_2$ .



## References

- (1) Payne, M. C.; Teter, M. P.; Allan, D. C.; Arias, T. A.; Joannopoulos, J. D., *Rev. Mod. Phys.* 1992, 64, 1045- 1097.
- (2) Clark, S. J.; Segall, M. D.; Pickard, C. J.; Hasnip, P. J.; Probert, M. J.; Refson, K.; Payne, M. C., *Z. Kristallogr.* 2005, 220, 567-570.
- (3) Kohn, W., *Rev. Mod. Phys.* 1999, 71, 1253-1266.
- (4) Rappe, A. M.; Rabe, K. M.; Kaxiras, E.; Joannopoulos, J. D., *Phys. Rev. B* 1990, 41, 1227-1230.
- (5) Perdew, J. P.; Burke, K.; Ernzerhof, M., *Phys. Rev. Lett.* 1996, 77, 3865-3868
- (6) Monkhorst, H. J.; Pack, J. D., *Phys. Rev. B* 1976, 13, 5188-5192.
- (7) Kang, L.; Ramo, D. M.; Lin, Z.; Bristowe, P. D.; Qin, J.; Chen, C., *J. Mater. Chem. C* 2013, 1, 7363-7370.
- (8) Lin, J.; Lee, M. H.; Liu, Z. P.; Chen, C. T.; Pickard, C. J., *Phys. Rev. B* 1999, 60, 13380-13389.
- (9) Woo, K.; Wang, J.; Mark, J.; Kovnir, K., *J. Am. Chem. Soc.* 2019, 141, 13017-13021.